Features of electron scattering in δ-doped GaAs/GaAlAs multiquantum well structures

A. de Visser, V. I. Kadushkin, V. A. Kul'bachinshkiĭ, V. G. Kytin, V. M. Skorokhodov, and E. L. Shangina

M. V. Lomonosov Moscow State University, 119899 Moscow, Russia

(Submitted 20 January 1994)
Zh. Eksp. Teor. Fiz. **105**, 1701–1713 (June 1994)

The temperature dependence of the conductivity, negative magnetoresistance, Shubnikov–de Haas effect, and quantum Hall effect in modulation-doped and δ-doped GaAs/GaAlAs multiquantum well structures have been investigated in the temperature range $0.39 < T < 300$ K. The dependences of the mobility on the quantum-well width, the distance from the δ layer to the quantum well, and the temperature have been determined and attributed to the interface-roughness scattering of electrons on the lateral surfaces of the quantum wells. The phase relaxation time τ_φ of the electronic wave function and its temperature dependence have been determined by analyzing the negative magnetoresistance according to the theory of quantum corrections to the conductivity for the two-dimensional case. It has been shown that the concentration of two-dimensional electrons in narrow quantum wells and their mobility are higher in the δ-doped structures than in the modulation-doped quantum wells.

1. INTRODUCTION

Doped superlattices and systems of quantum wells have been the subject of fervent theoretical and experimental investigations.[1,2] Single quantum wells and multiquantum well (MQW) systems are exceptionally convenient objects for investigating the relaxation mechanisms of two-dimensional ($2D$) electrons and the features of their interaction with excitations of various kinds and with crystal-lattice defects.[3,4] Advances in molecular-beam epitaxy have made it possible to obtain MQW systems with widely variable parameters. This method can be used to obtain sharp interfaces and fairly smooth surfaces. Historically, attention was first focused on superlattices by predictions of anomalous transport properties, particularly a negative differential conductivity. However, significant progress was subsequently achieved in the study and utilization of the optical properties of semiconductor superlattices and MQW systems. One of the promising practical outcomes has been the creation of IR photodetectors for the 8–14 μm wavelength range on the basis of superlattices and MQW systems.[5] The photoelectric characteristics of such devices are largely determined by the perfection of the structure, and any lattice imperfections (whether regular or random) can serve as recombination channels, which lower the quantum efficiency and worsen the noise characteristics. The doping method selected for creating $2D$ electrons in a quantum well is an important issue. Modulation doping of a quantum well (GaAs in a GaAs/AlGaAs system) by a donor impurity is associated with roughening of the GaAs(Si)/AlGaAs interface as a result of partial doping of the barrier layers by the diffusion of silicon, as well as fluctuations in the ground state energy due to the potential of the impurity atoms. In addition, there is a channel for a dark current along the impurity states (when there is weak overlapping of the electronic wave functions) or by means of hopping conduction (when the quantum wells are adequately spaced). These problems can be eliminated by δ-doping the AlGaAs layers with silicon. In this case the ionized impurities are spatially separated from the conducting channel by a spacing analog, which should have a significant influence on the transport phenomena.

The mechanism of the scattering of charge carriers in MQW systems can be studied by both optical and galvanomagnetic methods. In particular, investigations of photoluminescence spectra have shown that the lines broaden upon doping. The perfection of the interfaces, especially in narrow quantum wells, the distribution of ionized impurities, and other such factors should play a significant role in the scattering of electrons.

The aims of the present research were to study low-temperature transport in GaAs/$Ga_{1-x}Al_xAs$(δ-Si) MQW systems with a δ-doped barrier and different distances from the δ layer to the well boundary, as well as to compare their electrophysical properties with a GaAs(Si)/GaAlAs MQW system with direct modulation doping of the quantum wells.

2. SAMPLES AND MEASUREMENT METHOD

Two series of MQW structures grown by molecular-beam epitaxy were investigated. The MQW's of the first type were structures consisting of 50 periods of i-$Al_xGa_{1-x}As$ barriers ($x=0.30$) with a thickness of 25.4 nm and quantum wells with a width $L_W=3.3$–6.6 nm, which were modulation-doped by silicon to the 2×10^{18} cm^{-3} level. In the samples of the second type a δ layer of silicon was grown in the i-$Al_xGa_{1-x}As$ barrier of each period at a distance $L_\delta=3.0$–7.4 nm from the heterointerface. The width of the quantum wells was 5.1 nm, and the width of the barrier was 25 nm. The MQW structures were separated from the GaAs(Cr) substrate by an i-$Al_xGa_{1-x}As$ buffer layer with a thickness of 1 μm and had n^+-GaAs contact layers, which are needed to employ

 1063-7761/94/060918-08$10.00

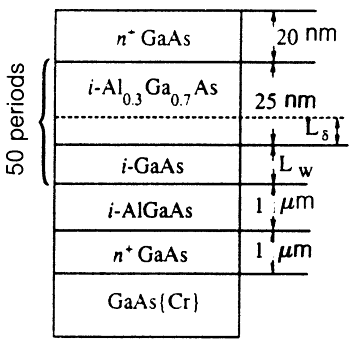

FIG. 1. Diagram of δ-doped MQW structures.

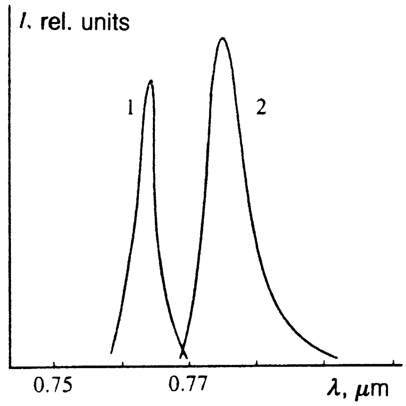

FIG. 2. Typical photoluminescence spectra of MQW structures with δ-doped barriers (curve *1*, sample N3) and modulation-doped barriers (curve *2*, sample N7).

these structures as photodetectors. It seemed important to investigate the features of electron scattering specifically in the structures with contact layers, which are employed directly as photodetectors. The choice of the GaAs-$Ga_{1-x}Al_xAs$(δ-Si) MQW system with $L_W=5.1$ nm for the investigation was governed by the fact that when $x=0.3$ the excitation of $2D$ electrons from the dimensional quantization level upon vertical transport corresponds to 8–12 μm radiation. A value in the range $L_W<6$ nm is the cut-off value separating narrow and broad quantum wells with different electron scattering mechanisms,[3,4] which will be discussed in greater detail below.

A schematic representation of the structure of the δ-doped samples is shown in Fig. 1. The samples for the measurements were prepared in the form of a double Hall bridge with a channel width of 150 μm. The temperature dependence of the conductivity in the 0.39–300 K temperature range, as well as the Hall effect and the transverse magnetoresistance in the 0.39–25 K range, were measured. Some parameters of the samples investigated are presented in Table I. The concentrations of $2D$ electrons per quantum well are indicated. The contact layers could be excluded from the calculations of the concentrations and Fermi energies of the $2D$ electrons in all the samples, since the electron concentrations and mobilities in these layers were measured. Table I gives the integral values of the mobility from the Hall effect for samples 1–4 and the mobilities of $2D$ electrons for samples 5–8. Magnetic fields with strengths up to 8 T were created with the aid of a hot-field superconducting solenoid. Magnetic fields with strengths up to 40 T were obtained with the aid of the system for producing quasi-stationary magnetic fields of Amsterdam University (the pulse duration was as long as 2 s.[6] An He^3 vapor pumping system was used to obtain temperatures down to 0.39 K.

3. MEASUREMENT RESULTS

The structural perfection of the MQW samples was quite good, the half-width of the photoluminescence spectrum at $T=4.2$ K being 13–21 meV for the modulation-doped samples (Fig. 2).

The MQW systems exhibited highly nonlinear current-voltage characteristics. The dependence of the conductivity on the electric field E contains segments which can be

TABLE I. Parameters of samples at $T=4.2$ K.

№	L_W, Å (L_δ, Å)	E_F, meV	n_1, 10^{11} cm^{-2}	μ, cm^2/Vs	D, cm^2/s	δE, meV	δE_0, meV	$\beta^* \cdot 10^{-2}$, (cm/V)^2
1	51(30)	31	9	1340	—	6	6.5	0.4
2	51(44)	34	10	1100	—	6	6.5	0.2
3	51(59)	37	10.8	1640	203	9	6.5	2.0
4	51(74)	24	7.1	1730	119	5	6.5	< 0.1
5	33	23	6.5	260	7.2	21	30	0.9
6	44	15	4.3	480	8.8	13	16	0.2
7	55	6.8	1.9	12	0.1	19	10	3.0
8	66	92	25.7	860	79	15	7	1.0

Note: 1–4—δ-doped samples; 5–8— modulation-doped samples. L_w is the well width, L_δ is the distance from the δ layer to the heterointerface, E_F is the Fermi energy, D is the diffusion coefficient, μ is the mobility, δE is the half-width of the photoluminescence peak, δE_0 is the fluctuation of the ground-state energy in a quantum well, and n_1 is the electron concentration in one quantum well.

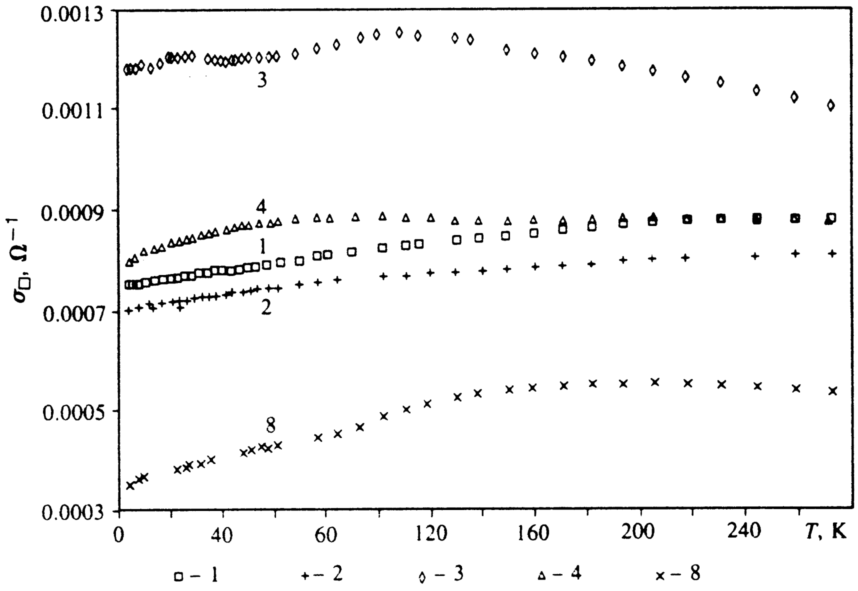

FIG. 3. Temperature dependence of the conductivity per square. The numbers on the curves correspond to the numbers of the samples in Table I.

approximated by the expression $\sigma=\sigma_0(1+\beta^*E^2)$. The values of β^* are presented in Table I. They differ from the values known for $2D$ electrons in heterojunctions,[7] but are very close to the values in an $Si–SiO_2$ system with strong manifestations of localization effects.[8]

Figure 3 presents plots of the temperature dependence of the conductivity per square for some MQW structures. The numbers on the curves correspond to the numbers of the samples in Table I. The conductivity of all the MQW systems decreases as the temperature decreases from room temperature to 4.2 K. At temperatures below 20 K the dependence of $\sigma(T)$ is approximated well by a logarithmic temperature dependence. The conductivity of the modulation-doped samples (the dependence for sample 8 is presented in Fig. 3 as an example) is lower than the conductivity of the δ-doped samples. The temperature dependence of the conductivity has a smaller slope in the case of the δ-doped samples. The mobility in the modulation-doped samples increases with the well width. A tendency for an increase in the mobility with increasing distance L_δ from the δ layer to the heterointerface can be traced for the δ-doped samples.

At low temperatures all the samples exhibit a negative magnetoresistance, which is quadratic in weak magnetic fields and logarithmically dependent on the magnetic field strength in strong fields. As the temperature rises, the range with a quadratic dependence of the negative magnetoresistance on the magnetic field broadens, the magnetic field strength at the onset of the logarithmic dependence increases, and the absolute value of the negative magnetoresistance decreases. Figure 4 presents plots of the dependence of the relative change in conductivity on the magnetic field strength for samples 3 and 4 at various temperatures. At higher temperatures the magnetoresistance becomes positive and exhibits a quadratic dependence on the magnetic field. An investigation of the Hall effect showed that the concentration of 2D electrons in both the GaAs/AlGaAs(δ-Si) and GaAs(Si)/AlGaAs structures is nearly independent of the temperature in the temperature range investigated. The absolute value of the negative magnetoresistance is greater in the modulation-doped samples. Figure 5 presents the relative changes in conductivity in a magnetic field for the δ-doped (curves *2–4*) and modulation-doped (curves *5* and *8*) samples.

At low temperature all the samples exhibited the Shubnikov–de Haas effect and the quantum Hall effect. Figure 6(a) presents the oscillations of the transverse magnetoresistance ρ_{xx} in sample 1 at $T=0.4$ K, and Fig. 7(a) presents the oscillations of ρ_{xx} and of the Hall resistance ρ_{xy} in sample 3 at $T=4.2$ K. One special feature of these oscillations is the presence of two frequencies in the spectrum. This phenomenon is attributed to the fact that oscillations are observed not only from the $2D$ electrons, but also from the contact layers, which are clearly distinguishable upon Fourier transformation [see local maximum 1 in Figs. 6(b) and 7(b)]. The electron concentration in the contact layers was thus determined.

4. DISCUSSION OF RESULTS

One significant difference between the two doping methods is the greater structural perfection of the δ-doped samples, as is evidenced by the smaller width of the photoluminescence spectra (see Fig. 2 and Table I). The electron concentration and mobility are greater in the δ-doped MQW systems.

The electron mobility in the samples investigated increases fairly rapidly as the quantum-well width increases.

A model of the interface-roughness (IFR) scattering of electrons on the lateral surfaces of quantum wells was proposed in Ref. 3 to understand and explain the decrease in mobility observed as the well width decreases. The electron mobility in quantum wells and its dependence on the well width can be calculated numerically.[3,4,9,10] As follows from the data presented, our results are described well by the IFR scattering of electrons in quantum wells. Confir-

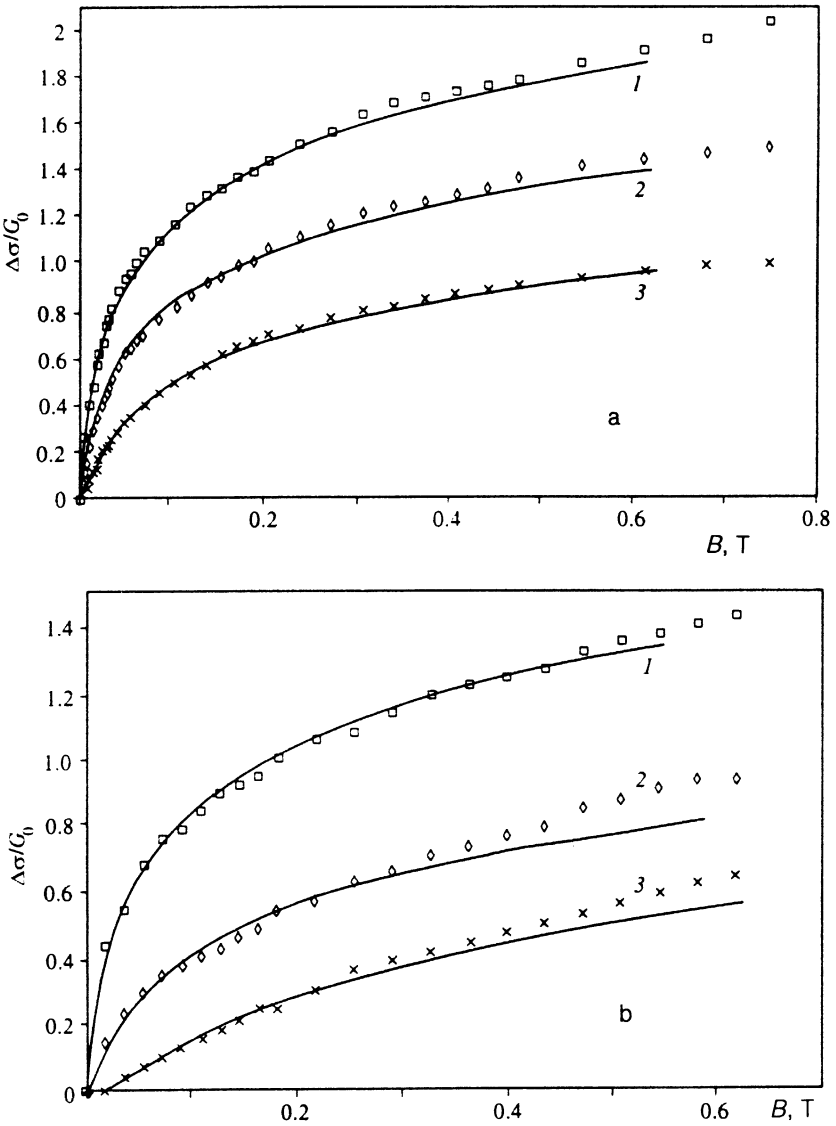

FIG. 4. Dependence of the reduced conductivity on the magnetic field for samples 3(a) and 4(b) at various temperatures T, K. a: *1*) 4.2; *2*) 10; *3*) 17. b: *1*) 4.2; *2*) 10; *3*) 17. The points represent experimental values, and the solid lines represent values calculated from Eq. (5). $G_0 = 1.23 \cdot 10^{-5}\ \Omega^{-1}$.

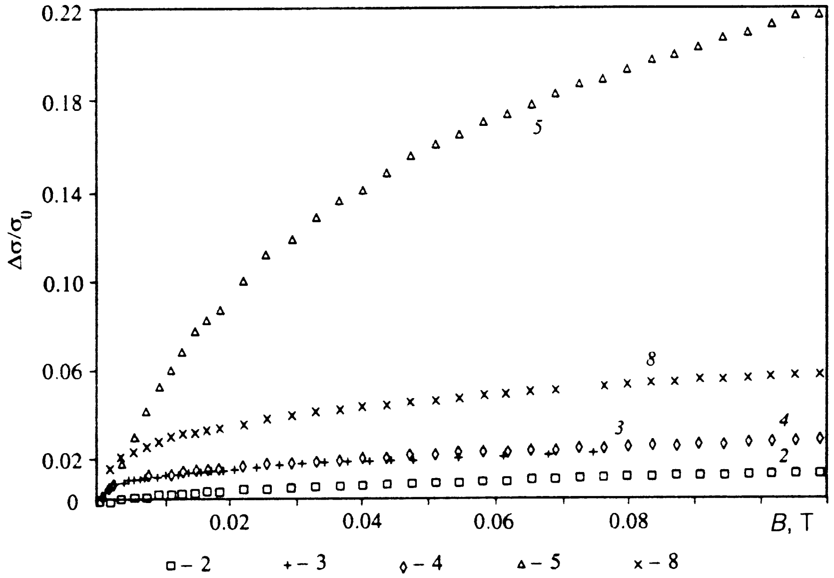

FIG. 5. Relative change in the conductivity of samples in a magnetic field for various distances of the δ layer from the heterointerface of the quantum well (curves *2*–*4*). For comparison, the corresponding dependences for δ-doped samples are presented (curves *5* and *8*). $T = 4.2$ K. The numbers correspond to Table I.

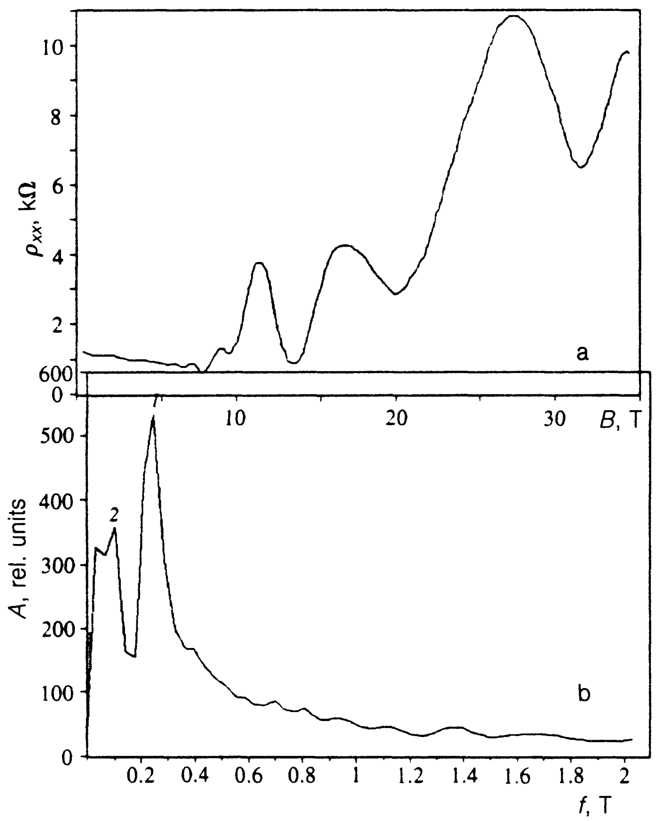

FIG. 6. Shubnikov–de Haas oscillations of ρ_{xx} in sample 1 at $T=0.4$ K (a) and their Fourier transform (b): *1*) oscillations from the contact layers; *2*) $2D$ electrons.

mation of the predominance of this scattering mechanism is provided by the temperature dependences of the mobility calculated for modulation-doped GaAs(Si)/AlGaAs quantum wells in Ref. 10. In the present study we calculated the temperature dependences of the mobility for δ-doped GaAs/AlGaAs(δ-Si) MQW structures with predominant scattering of the charge carriers on ionized impurities and with predominant IFR scattering. In the former case we used the calculation procedure published in Ref. 7. The mobility values obtained were approximately an order of magnitude higher than the experimental values and exhibited a different temperature dependence. In the latter case the mobility is given by the expression[3,9]

$$\mu=\frac{L_W^6 g(\Lambda,T,n)}{\Lambda^2\Delta^2}, \tag{1}$$

where $g(\Lambda,T,n)$ is a smooth function of the lateral size of the quantum-well roughness Λ, the temperature T, and the concentration of charge carriers n. The mobility calculated from Eq. (1) is strongly dependent on the well width, in good agreement with the experimental results (see Table I). The calculated temperature dependences of the mobility can be fitted to the experimental plots by varying the height and lateral size of the roughness. The values of the mobility $\mu=R_x\sigma$ listed in Table I for δ-doped samples 1–4 were obtained from experimental values of the conductivity σ and the Hall coefficient R_x. To compare the experimental data with theory, the values of the mobility and the concentration n_1 of $2D$ electrons in the quantum wells were calculated from the Shubnikov–de Haas oscillations. The procedure used to perform such calculations was described in Refs. 11 and 12. It involves Fourier transformation, separation of the frequencies, and the performance of inverse Fourier transformation for each frequency. After inverse transformation, the oscillations have a single frequency, and the mobility is easily determined from them. The values of $\mu_{\exp}$ for the $2D$ electrons thus determined are presented in Table II. We note that there is no fine structureon the plateau of the quantum Hall effect for the samples investigated (see Figs. 6 and 7) and that the oscillations from the $2D$ electrons are monochromatic, attesting to the identical nature of the 50 quantum wells grown. The mobility under the assumption of IFR scattering was calculated for samples 3 and 4. The best agreement with the experimental plots of the temperature dependence of the mobility was obtained for a roughness height $\Delta=2.83$ Å (which corresponds to the height of a single layer) and $\Lambda=11$ nm (sample 3) or $\Lambda=15$ nm (sample 4). According to the photoluminescence data, the half-width δE of the ground-state emission line of undoped samples with the same parameters (analogs of the doped samples) at 4.2 K was ≈ 5 meV, which corresponds to the roughness height and lateral size obtained from fitting the dependences of $\mu(T)$. The fluctuations of the ground-state energy in a quantum well δE_0 caused by the interface roughness and the values of δE for the samples investigated are listed in Table I. The two sets of values are in good agreement.

Analysis of the temperature dependences of the conductivity (see Fig. 3) and of the negative magnetoresistance (see Fig. 4) provides a method for determining the characteristic relaxation times of the charge carriers, particularly the phase relaxation time τ_φ of the wave function due to quasi-elastic electron scattering. The value of τ_φ is determined by electron–electron or electron–phonon interactions (we shall not consider the inelastic times associated with spin-flip scattering or with intervalley scattering). The relationship of τ_φ to the characteristic time of inelastic collisions and the energy relaxation time was examined in Refs. 13 and 14.

At low temperatures the logarithmic increase in resistance observed as the temperature is lowered and the negative magnetoresistance, which is quadratic in weak and logarithmic in strong magnetic fields, are accurately described by the theory of quantum corrections to the conductivity for the two-dimensional case,[13–15] which holds in the degeneracy region, i.e., when $E_F \gg kT$. When the temperature is varied, the conductivity σ then varies according to the law

$$\sigma(T_2)-\sigma(T_1)=A\frac{e^2}{2\pi^2\hbar}\ln(T_2/T_1). \tag{2}$$

The coefficient A in the logarithmic temperature dependence of the conductivity is determined by both the weak localization and the electron–phonon interaction:

$$A=\beta+(1-\beta)p+\Lambda, \tag{3}$$

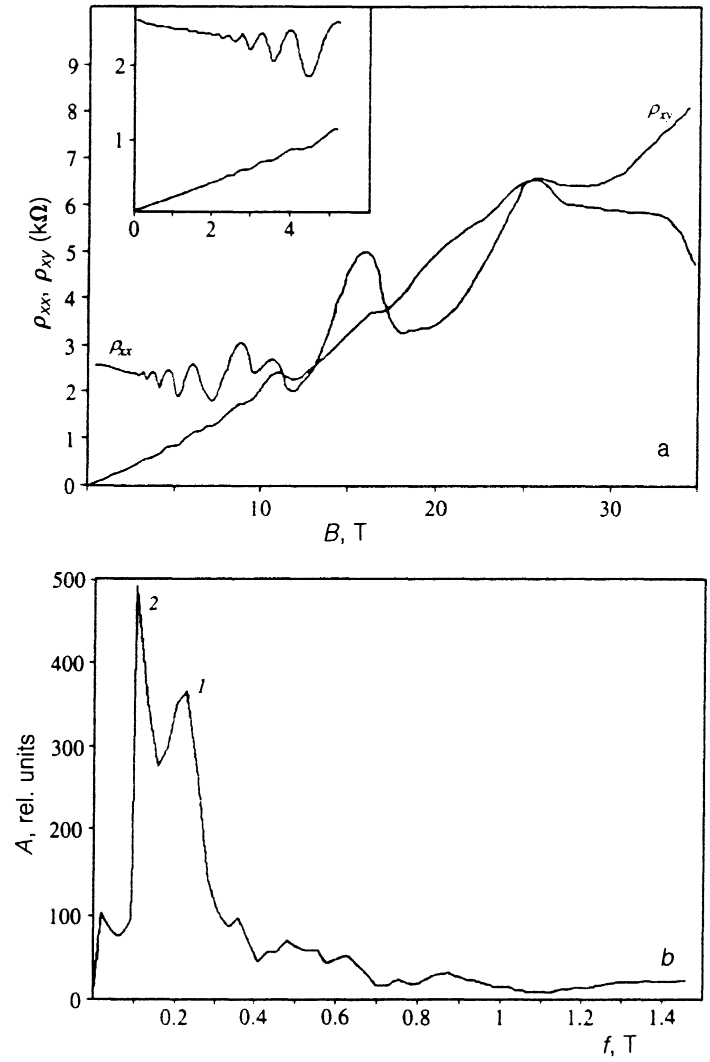

FIG. 7. Shubnikov–de Haas oscillations of ρ_{xx} and the Hall resistance ρ_{xy} of sample 3 at $T=4.2$ K (a) and their Fourier transform (b). *1*) oscillations from the contact layers; *2*) from $2D$ electrons. Plots of ρ_{xx} and ρ_{xy} in weak magnetic fields are given in the insert.

where p is the exponent in the dependence of τ_φ on the temperature[13,14]

$$\tau_\varphi = aT^{-p} \tag{4}$$

and Λ is the electron–electron interaction constant in the diffusion channel.

The variation of the conductivity in a magnetic field is described by the equation

$$\sigma(B)-\sigma(0)=\frac{e^2}{2\pi^2\hbar}(1-\beta)f_2\left(\frac{4DeB\tau_\varphi}{\hbar c}\right), \tag{5}$$

where D is the diffusion coefficient, $f_2(x)$ has asymptotes equal to $x^2/24$ at $x \ll 1$ and to $\ln x$ at $x \gg 1$.[15,16] The coefficient β takes into account the Maki–Thompson correction associated with scattering on superconducting fluctuations. As was shown in Ref. 17, dependence (5) holds as long as the magnetic length $l_B=(\hbar c/eB)$ is greater than the free path l of the electrons. In the samples investigated in the present work the electron mobility is not very high, permitting the employment of Eq. (5) in the magnetic fields used in the present study for the calculations ($B<1$ T). A

TABLE II. Some parameters of the $2D$ electrons in samples 3 and 4 at $T=4.2$ K.

No.	E_F, meV	n_1, 10^{11} cm^{-2}	$\mu_{\rm exp}$, cm^2/Vs	$\mu_{\rm calc}$, cm^2/Vs	Λ, nm	$E_{1\rm exp}$, eV	$E_{1\rm calc}$, eV
3	37	10.8	5500	5370	11	1.625	1.622
4	24	7.1	5000	4860	15	1.629	1.623

Here E_F is the Fermi energy, n_1 is the concentration of $2D$ electrons, $\mu_{\rm exp}$ and $\mu_{\rm calc}$ are the experimental and calculated values of the mobility, $E_{1\rm exp}$ and $E_{1\rm calc}$ are the experimental and calculated values of the optical transition energy, and Λ is the lateral size of the roughness.

TABLE III. Temperature dependence of τ_φ for samples 3 and 4.

T,K	τ_φ, 10^{-12} sec	
	3	4
4.2	12.0	16.0
6.0	–	7.6
10	7.3	5.0
17	3.2	1.0

magnetic field disrupts weak localization and suppresses the corresponding contribution to (5). A dependence of λ on the magnetic field should be displayed when $g\mu_B B/kT > 1$ (μ_B is the Bohr magneton); therefore, this dependence may be disregarded in our case at low temperatures. The contributions from weak localization and the electron–electron interaction can generally be separated, as was done for a $2D$ electron gas at ultralow temperatures in Ref. 18. An analysis of the experimental data can be performed without taking into account the quantum correction associated with the interaction of electrons in the Cooper channel,[13] making it possible to fully describe the galvanomagnetic phenomena in a $2D$ electron gas.[19] Use of the Einstein formula for a degenerate electron gas

$$\mu = eD/E_F \tag{6}$$

and the values of the mobility of $2D$ electrons in the framework of the assumptions made gives the values of the diffusion coefficient in Table I. Then the negative magnetoresistance can be fitted to the experimental data in Fig. 4, using τ_φ as a parameter in (5). The result of such treatment is illustrated by the solid lines in Fig. 4. The temperature dependence of τ_φ can hence be obtained. It is presented in Table III. As follows from our data, $\tau_\varphi(T)$ is described well by Eq. (4) with $p=1$ in both types of MQW structures. This means that the main phase relaxation mechanism in the systems investigated at low temperatures is based on electron–electron collisions with small energy transfer.[20] The value of τ_φ depends on the quantum-well width L_W, increasing with increasing L_W in both the GaAs/GaAlAs(δ-Si) and GaAs(Si)/GaAlAs structures.

An investigation of the features of the Shubnikov–de Haas oscillations of the δ-doped MQW systems reveals that we are dealing with a system in which only the lowest-lying subband is filled. We calculated the band diagram of the δ-doped structures. A pair of adjacent quantum wells formed in δ-Si and GaAs was regarded as a single quantum-mechanical system in the calculation. Such a treatment was performed in view of the fact that L_δ is smaller than the Bohr radius of the electron in the impurity in GaAlAs. The calculation was based on self-consistent solution of the Schrödinger and Poisson equations using the procedure published in Ref. 21. The concentration of donors (Si) in the plane of the δ layer needed for the calculation was set equal to the two-dimensional concentration of charge carriers n_1 in a single filled subband obtained from the Shubnikov–de Haas oscillations. The band diagram was calculated for $T=4.2$ K with a boundary band offset parameter equal to 0.6 and a quadratic dispersion law. The band diagram thus obtained for sample N3 is presented in Fig. 8.

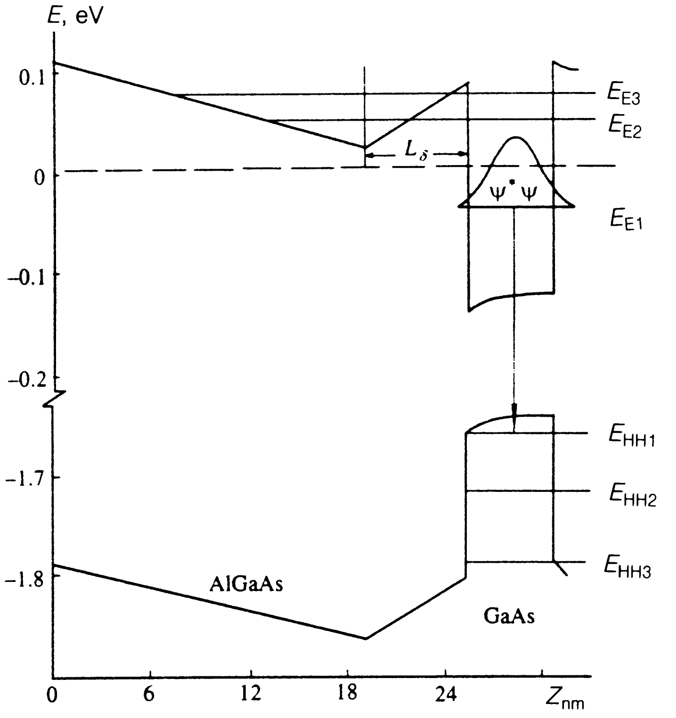

FIG. 8. Typical energy band diagram of the periodically repeated portion of δ-doped structure N3. The dashed line corresponds to the level of the chemical potential. E_c is the bottom of the conduction band, and E_v is the top of the valence band. A profile of the normalized wave function of the electronic ground state is shown. The $E1$–$HH1$ transition with an energy E_{H1}, which is observed in the photoluminescence spectra, is indicated by the arrow.

According to the calculation, at an electron concentration $n_1 < 10^{12}$ cm^{-2}, only one subband is filled in the system of coupled quantum wells formed by the GaAs and δ(Si) layers. The wave function corresponding to this subband is localized in the GaAs layer.

The photoluminescence spectra of the structures investigated exhibit $E1$–$HH1$ transitions, which are caused by the recombination of free carriers, viz., an electron and a heavy hole. The empirical transition energy $E_{1\,\mathrm{exp}}$ is close to the calculated value $E_{1\,\mathrm{calc}}$ (see Fig. 8 and Table II). The half-width of the photoluminescence spectra falls in the 5–9 meV range, which corresponds to fluctuations of the ground-state energy caused by a change in the quantum-well width $L_W=5.1$ nm by one monolayer due to the island character of the heterointerface.

5. CONCLUSIONS

Thus, the body of experimental data allows us to conclude that the dependences of the electron mobility in the GaAs/GaAlAs MQW systems investigated on the well width and the temperature at low temperatures may be attributed to the interface-roughness scattering of electrons regardless of the doping method. The galvanomagnetic properties of the superlattices are described at low temperatures by the theory of quantum corrections to the conductivity, which revealed that the main mechanism for phase relaxation of the electronic wave function in the systems investigated at low temperatures is based on electron-electron collisions with small energy transfer.

The samples of δ-doped barriers have greater structural perfection and greater mobility of the $2D$ electrons than do the modulation-doped samples. Such an effect was previously observed in systems with δ-doped quantum wells.[22]

MQW systems with δ-doped barriers are promising for use as IR photodetectors with a larger quantum yield, better selectivity, and a gain in thickness of the photosensitive region in comparison with the known modulation-doped structures.[5]

[1] A. P. Silin, Usp. Fiz. Nauk **147**, 485 (1985) [Sov. Phys. Usp. **28**, 972 (1985)].

[2] K. Ploog and G. H. Döhler, Adv. Phys. **32**, 285 (1983).

[3] K. Hirakawa, T. Noda, and H. Sakaki, Surf. Sci. **196**, 365 (1988).

[4] T. Noda, M. Tanaka, and H. Sakaki, Appl. Phys. Lett. **57**, 1651 (1990).

[5] B. F. Levine, C. G. Bethea, G. Hasnain, J. Walker, and P. J. Malik, Appl. Phys. Lett. **53**, 296 (1988).

[6] R. Gersdorf, F. R. de Boer, J. C. Wolfrat, F. A. Muller, and L. W. Roeland, in *High Field Magnetism*, edited by M. Date, North-Holland, Amsterdam (1983), p. 277.

[7] T. Ando, A. B. Fowler, and F. Stern, "Electronic properties of two-dimensional systems," Rev. Mod. Phys. **54**, 437–672 (1982) (Russ. transl. Mir, Moscow, 1985).

[8] V. I. Kadushkin and E. L. Shangina, Fiz. Tekh. Poluprovodn. **27**, 1311 (1993) [Semiconductors **27**, 725 (1993)].

[9] H. Sakaki, T. Noda, K. Hirakawa, M. Tanaka, and T. Matsusue, Appl. Phys. Lett. **51**, 1934 (1987).

[10] V. A. Kulbachinskii, V. G. Kytin, V. I. Kadushkin, E. L. Shangina, and A. de Visser, J. Appl. Phys. **75**, 2081 (1994).

[11] S. Yamada and T. Makimoto, Appl. Phys. Lett. **57**, 1022 (1990).

[12] P. M. Koenraad, B. F. A. van Hest, F. A. P. Blom, R. van Dalen, M. Leys, J. A. A. J. Perenboom, and J. H. Wolter, Physica B **177**, 485 (1992).

[13] B. L. Altshuler and A. G. Aronov, in *Modern Problems in Condensed Matter Sciences, Vol. 10, Electron-Electron Interactions in Disordered Systems*, edited by A. L. Efros and M. Pollak, North-Holland, Amsterdam, 1985, pp. 1–153.

[14] A. G. Aronov, Physica B **126**, 314 (1984).

[15] B. L. Al'tshuler, A. G. Aronov, A. N. Lapkin, and D. E. Khmel'nitskiĭ, Zh. Eksp. Teor. Fiz. **81**, 768 (1981) [Sov. Phys. JETP **54**, 411 (1981)].

[16] T. A. Polyanskaya and Yu. B. Shmartsev, Fiz. Tekh. Poluprovodn. **23**, 3 (1989) [Sov. Phys. Semicond. **23**, 1 (1989)].

[17] V. M. Gasparyan and A. I. Zyuzin, Fiz. Tverd. Tela **27**, 1662 (1985) [Sov. Phys. Solid State **27**, 999 (1985)].

[18] B. J. F. Lin, M. A. Paalanen, A. C. Gossard, and D. C. Tsui, Phys. Rev. B **29**, 927 (1984).

[19] I. G. Savel'ev and T. A. Polyanskaya, Fiz. Tekh. Poluprovodn. **22**, 1818 (1988) [Sov. Phys. Semicond. **22**, 1150 (1988)].

[20] B. L. Altshuler, A. G. Aronov, and D. E. Khmelnitsky, J. Phys. C **36**, 7367 (1982).

[21] A. K. Ghatak, K. Thyagarajan, and M. R. Shenoy, IEEE J. Quantum Electron. **24**, 1524 (1988).

[22] S. Sasa, K. Kondo, H. Ishikawa, T. Fujii, S. Muto, and S. Hiyamizu, Surf. Sci. **174**, 433 (1986).

Translated by P. Shelnitz